Article

Utilization of Emulsion Inversion to Fabricate Tea (*Camellia sinensis* L.) Flower Extract Obtained by Supercritical Fluid Extraction-Loaded Nanoemulsions

Nara Yaowiwat,* Worrapan Poomanee, Pimporn Leelapornpisid, and Phanuphong Chaiwut

Read Online

ACCESS | Metrics & More | Article Recommendations

ABSTRACT: This study aimed to obtain tea flower extract (TFE) using supercritical fluid extraction, to determine the compounds present in the TFE and to establish its antioxidant activity. The fabrication of TFE nanoemulsions was also investigated using response surface methodology (RSM). UHPLC-ESI-QTOF-MS/MS and UHPLC-ESI-QqQ-MS/MS analysis showed that the TFE was composed of catechin and its derivatives, flavonols and anthocyanins, suggesting its potential as a free radical scavenger with strong reducing powers. A central composite design was applied to optimize the independent factors of the nanoemulsions. The factors had a significant ($p < 0.05$) effect on all response variables. The optimum level of factors for the fabrication was a surfactant-to-oil ratio of 2:1, a high hydrophilic−lipophilic balance (HLB) surfactant to low HLB surfactant ratio (HLR) of 1.6:1, and a PEG-40/PEG-60 hydrogenated castor oil ratio of 2:1. The responses obtained from the optimum levels were a 34.01 nm droplet size, a polydispersity index of 0.15, and 75.85% entrapment efficiency. In conclusion, TFE could be an antioxidant active ingredient and has been successfully loaded into nanoemulsions using RSM.

Dried tea (*Camellia sinensis* L.) flowers — Supercritical fluid extraction — Tea (*Camellia sinensis* L.) flower extract — TFE loaded nanoemulsions
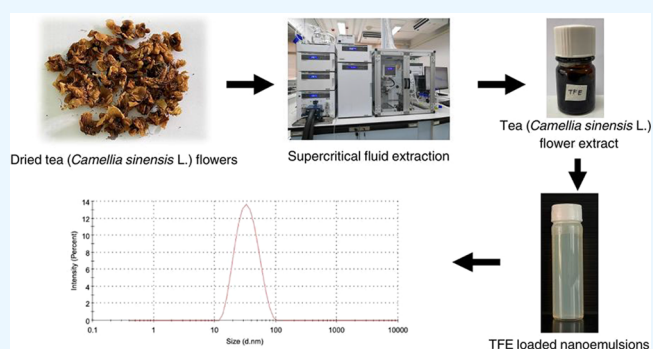
1. INTRODUCTION

Tea flowers, a naturally plentiful resource, are completely flowered, which could be reproduced without recultivation.[1,2] In the past, tea flowers were considered to be a waste product in the agricultural process, because manufacturers and consumers focused on the tea leaves and buds due to their various health benefits. In recent years, tea flowers have become more interesting, with several researchers reporting that they are as valuable as tea leaves.[1,2] Previously, many studies have reported that the antioxidant effects of galloylated catechins were stronger than those of nongalloylated catechins and that the effects of [(−)-epigallocatechin] were also stronger than those of [(−)-epi-catechin] and [(+)-catechin].[3] Grzesik et al. also found (−)-epigallocatechin gallate to be the most effective as it had the highest antiradical capacity.[4] Tea flowers also contain flavonols in several forms, especially in the form of glycosides, including kaempferol, quercetin, and myricetin, which are a main class of flavonoids.[1,2] Many studies have also demonstrated that tea flowers have various kinds of potential health benefits, such as antioxidant, immune-stimulating, and anti-inflammatory activities.[1]

Many researchers have investigated nanoencapsulation technology to protect the bioactivity and bioactive compounds of tea flowers, because it overcomes the instability of bioactive compounds, reduces unpleasant taste or flavors, and also enhances permeability.[5−9] Nanoemulsions are lipid-based nanoparticles consisting of an oil phase mixed with an aqueous phase containing an appropriate ratio of surfactant.[8] Nanoemulsions can be fabricated using different techniques, which can be mainly classified as either high energy or low energy emulsifications.[8]

The aim of this study was to fabricate oil-in-water nanoemulsions containing tea flower extract (TFE) and to evaluate the effects of the emulsifying conditions on the response variables, including the droplet size, size distribution, and entrapment efficacy. The bioactive composition of the TFE and its antioxidant activity were also investigated.

Table 1. Bioactive Compounds Identified in TFE by UHPLC-ESI-QTOF-MS/MS

compound	RT (min)	molecular formular	m/z	mass (theoretical)	mass (experimental)	error (ppm)
caffeine	9.445	$C_8H_{10}N_4O_2$	195.0878	194.0804	194.0804	−0.24
CATECHINS						
(−)-catechin-4beta-ol	5.905	$C_{15}H_{14}O_7$	305.0667	306.074	306.074	−0.22
(+)-catechin-4beta-ol	8.396	$C_{15}H_{14}O_7$	305.0668	306.074	306.074	−0.37
(+)-gallocatechin	8.397	$C_{15}H_{14}O_7$	307.0814	306.074	306.074	−0.58
(−)-catechin	9.324	$C_{15}H_{14}O_6$	289.0718	290.079	290.079	−0.32
(+)-catechin	11.407	$C_{15}H_{14}O_6$	291.0866	290.079	290.079	−0.79
(−)-epigallocatechin gallate	11.601	$C_{22}H_{18}O_{11}$	457.0781	458.0849	458.0849	−0.82
(+)-epigallocatechin gallate	11.610	$C_{22}H_{18}O_{11}$	459.0921	458.0849	458.0849	−0.08
(−)-epigallocatechin 3-(3-methyl-gallate)	14.225	$C_{23}H_{20}O_{11}$	471.0933	472.1006	472.1006	−0.07
(+)-catechin 3′-O-gallate	15.989	$C_{22}H_{18}O_{10}$	443.0973	442.09	442.09	−0.13
FLAVONOIDS						
kaempferol 7-(3G-glucosylgentiobioside)	14.100	$C_{33}H_{40}O_{21}$	771.1986	772.2062	772.2062	0.31
kaempferol 3-rutinoside-4′-glucoside	15.432	$C_{33}H_{40}O_{20}$	755.2038	756.2113	756.2113	0.44
quercetin 3-beta-D-glucoside	16.142	$C_{21}H_{20}O_{12}$	465.1031	464.0955	464.0955	−0.7
kaempferol 3-rhamninoside	16.162	$C_{33}H_{40}O_{19}$	739.2092	740.2164	740.2164	0.17
kaempferol 7-galactoside 3-rutinoside	16.184	$C_{33}H_{40}O_{20}$	755.2044	756.2113	756.2113	−0.72
kaempferol 3-laminaribioside-7-rhamnoside	16.185	$C_{33}H_{40}O_{20}$	757.2191	756.2113	756.2113	−0.48
quercitrin	16.527	$C_{21}H_{20}O_{11}$	447.0939	448.1006	448.1006	−0.78
narirutin	16.620	$C_{27}H_{32}O_{14}$	579.1731	580.1792	580.1792	−2.2
ANTHOCYANINS						
5-carboxypyrano cyanidin 3-O-beta-glucopyranoside	16.527	$C_{24}H_{20}O_{13}$	515.0811	516.0904	516.0904	4.24
delphinidin-3-O-glucoside pyruvic acid	16.126	$C_{24}H_{20}O_{14}$	531.0753	532.0853	532.0853	5.38
petunidin-3-O-arabinoside	16.185	$C_{21}H_{20}O_{11}$	449.1077	448.1006	448.1006	0.12
petunidin 3-galactoside	16.589	$C_{22}H_{22}O_{12}$	477.1038	478.1111	478.1111	−0.14
cyanidin 3-(6″-acetylglucoside)	17.156	$C_{23}H_{22}O_{12}$	489.1041	490.1111	490.1111	−0.85
malvidin 3-glucoside-4-vinylcatechol	17.532	$C_{31}H_{28}O_{14}$	623.1402	624.1479	624.1479	0.42

Table 2. Contents of Bioactive Composition in the TFE by UHPLC-ESI-QqQ-MS/MS

composition	RT (min)	linear equation	correlation coefficient: R^2	concentration (ppm)
caffeine	3.627	$y = 48,366,330x + 2,049,601$	0.9990512	4.33 ± 0.64
caffeic acid	4.574	$y = 12,402,100x + 159497.3$	0.9997329	0.06 ± 0.01
protocatechuic acid	2.670	$y = 7007.355x + 6762.765$	0.8132233	82.52 ± 2.98
gallic acid	1.640	$y = 3,183,944x + 36054.58$	0.9996324	1.58 ± 0.05
p-coumaric acid	5.535	$y = 6,349,098x + 44423.86$	0.9995383	0.04 ± 0.01
ferulic acid	5.706	$y = 388346.4x + 13558.94$	0.9996573	0.16 ± 0.01
catechin	3.967	$y = 2,135,389x + 2950.069$	0.9994077	0.05 ± 0.01
epicatechin (EC)	4.763	$y = 1,426,047x + 24115.47$	0.9996847	0.14 ± 0.02
gallocatechin (GC)	2.386	$y = 1,182,815x + 25075.34$	0.9997533	0.12 ± 0.01
epigallocatechin (EGC)	3.494	$y = 2,307,225x + 3103.182$	0.9997687	0.16 ± 0.02
catechin gallate (CG)	5.647	$y = 3,066,125x + 11638.07$	0.9995410	1.75 ± 0.02
gallocatechin gallate (GCG)	5.067	$y = 7,645,719x − 68883.98$	0.9988892	0.02 ± 0.00
epigallocatechin gallate (EGCG)	5.065	$y = 3,942,501x − 39618.69$	0.9994777	2.59 ± 0.02

2. RESULTS AND DISCUSSION

2.1. Extraction of TFE. The TFE was a viscous semisolid with a greenish-brown color. The extraction yield was 17.06 ± 1.76%. Various studies have reported that supercritical fluid extraction (SFE) requires fewer newer technologies, has higher selectivity, and requires less time, particularly for tea catechin extraction.[10]

2.2. Total Phenolic Content and Total Flavonoid Content. The total phenolic content (TPC) and total flavonoid content (TFC) of the TFE were 102.77 ± 1.23 mg of gallic acid equivalents (GAE)/g of extract and 27.48 ± 2.18 mg of quercetin equivalents (QE)/g of extract, respectively. The observed phenolic and flavonoid content in the TFE was correlated to the chemical compositions of the TFE, which was reported by Chen et al.[2]

2.3. Bioactive Composition of TFE. The untargeted assessment of the bioactive compound profile of TFE was performed using UHPLC-ESI-QTOF-MS/MS. The identified compounds are listed in Table 1, along with their retention times, molecular formulas, and molecular weights (m/z). UHPLC-QTOF-MS2 tentatively characterized a total of 24 compounds in the TFE, as shown in Table 1.

The identities of the flavonoids and anthocyanins were obtained by matching the molecular m/z values from the UHPLC-ESI-QTOF-MS/MS. Eight flavonoids in the form of glycosides formed from the flavonoid were detected in the TFE, along with six anthocyanins (as shown in Table 1). The bioactive compounds found in the TFE were consistent with the data provided by Chen et al.[1,2] Therefore, it was hypothesized that the TFE may have beneficial health effects by functioning as an

effective antioxidant and could be used as a remedy in the prevention and treatment of various diseases and with regard to its antiaging properties.

The catechins were quantified by UHPLC-ESI-QqQ-MS/MS using calibration curves of the standards, as shown in Table 2. The group of catechin derivatives found in the TFE included catechin, epicatechin, epigallocatechin, gallocatechin, catechin gallate, gallocatechin gallate, and epigallocatechin gallate, and the contents were determined to be 0.05 ± 0.01, 0.14 ± 0.02, 0.12 ± 0.01, 0.16 ± 0.02, 1.75 ± 0.02, 0.02 ± 0.00, and 2.59 ± 0.02 ppm, respectively. Other phenolic acid compounds were also found to be present, including caffeic acid, protocatechuic acid, gallic acid, p-coumaric acid, and ferulic acid, with corresponding contents of 0.06 ± 0.01, 82.52 ± 2.98, 1.58 ± 0.05, 0.04 ± 0.01, and 0.16 ± 0.01 ppm, respectively. The TFE also consisted of 4.33 ± 0.64 ppm of caffeine. The concentration of the group of catechins was slightly higher than the data provided by Chen et al., especially with respect to epigallocatechin gallate,[1,2] which is the most abundant catechin derivative reported in green tea infusions and considered to be one of the most active compounds known for its antioxidant properties.[11]

2.4. Antioxidant Activities of the TFE. The antioxidant activity of the TFE and standards was investigated using the DPPH radical scavenging assay, whereas the reducing capacity was investigated using the ferric reducing antioxidant power (FRAP) assay. The results showed that the TFE possessed an IC_{50} value of 0.467 ± 0.011 mg/mL. Gallic acid showed the lowest IC_{50} value of 0.024 ± 0.001 mg/mL among the antioxidants, followed by ascorbic acid (0.038 ± 0.001 mg/mL), quercetin (0.051 ± 0.001 mg/mL), and catechin (0.053 ± 0.001 mg/mL), respectively. The antioxidant activity of the TFE was mostly related to the concentration of catechin and phenolic compounds. Various studies have reported that the antioxidant action of catechin and its derivatives are accepted in various systems[4] and also suggest that the scavenging effects of epigallocatechin are stronger than those of epicatechin and catechin. Furthermore, epigallocatechin gallate has the highest antioxidant capacity, which could be correlated to the antioxidant activities of the TFE.

The reducing capacity is another measure of the antioxidant power: the FRAP method measures the direct capacity to reduce ferric ions to ferrous ions. The TFE had a strong reducing power of 1.001 ± 0.001 mM Fe(II)/g, comparative to ascorbic acid (1.550 ± 0.001 mM Fe(II)/g), while catechin presented the highest reducing power (1.998 ± 0.001 mM Fe(II)/g). The presence of the hydroxyl group in the phenolic ring is the main factor of reactivity in the FRAP assay. Previous studies have shown that the reactivity of catechins in the FRAP assay confirms their ability to reduce metal ions due to the hydroxyl groups in the structure.[4] Moreover, caffeic acid, which is reported in the TFE, presents two hydroxyl groups, and its ester was also correlated to FRAP reactivity.[12]

2.5. Optimization of Nanoemulsions. *2.5.1. Fitting the Model.* The experimental results of the three response variables (the droplet size, polydispersity index (PDI), and entrapment efficiency (EE)) are presented in Tables 4 and 5. The obtained models significantly fitted all response variables and presented a high coefficient of determination (R^2), in the range of 0.8947−0.9977. These results confirmed that all values obtained from the experiment were in good agreement with the predicted values. The predicted values of the response variables were calculated using the coefficient of the polynomial equation. The analyses of

variance (ANOVA) indicated that the experimental data represent the quadratic polynomial model. The results confirmed that all parameters in the regression models had a probability (p) less than 0.001, thus there was no lack of fit, as shown in Table 3.

Table 3. Regression Coefficient, R^2, Adjusted R^2, and Probability Values for the Final Model Equation[a]

regression coefficient	droplet size (Y_1, nm)	PDI (Y_2)	entrapment efficiency (Y_3, %)
β_0	54.27	0.1325	67.05
X_1	−31.68	−0.0105	15.57
X_2	−8.49	−0.0412	6.28
X_3	5.03	0.0081	−1.93
X_1^2	12.71	0.0165	−7.03
X_2^2	6.51	0.0476	−1.98
X_3^2	2.4	0.0001	0.2349
X_{12}	0.58	−0.0581	−3.96
X_{13}	−0.3375	−0.0344	−0.0788
X_{23}	−0.715	0.0369	0.0612
R^2	0.9507	0.8947	0.9977
adjusted R^2	0.9063	0.7999	0.9956
regression (p-value)	<0.0001[b]	0.0008[b]	<0.0001[b]

[a]β_0 is a constant; X_1, X_2, and X_3 are the estimated regression coefficients for the main linear effects; X_1^2, X_2^2, and X_3^2 are the estimated regression coefficients for the quadratic effects; X_{12}, X_{13}, and X_{23} are the estimated regression coefficients for the interaction effects. X_1: surfactant-to-oil ratio (SOR), X_2: the ratio of high hydrophilic−lipophilic balance (HLB) surfactant to low HLB surfactant (HLR), X_3: the effect of PEG-40 and PEG-60 hydrogenated castor oil. [b]Indicates a significant term ($p < 0.05$).

2.5.2. Effects of Independent Variables on the Responses. The effects of different levels of independent variables on the responses are presented in Table 5.

2.5.2.1. Droplet Size. As shown in Table 4, the droplet size was mainly affected by the SOR, with linear ($p < 0.0001$) and quadratic ($p < 0.01$) effects. Increasing the surfactant concentration led to a decrease in the droplet size. Another factor that significantly affected the linear ($p < 0.01$) and quadratic ($p < 0.01$) effects was the HLR, as shown in Table 4. The droplet size decreased as the HLR increased. Therefore, the main factors related to the physicochemical parameters are the oil/surfactant/water ratio and the surfactant blend.[13,14]

2.5.2.2. Polydispersity Index. As shown in Table 4, the HLR is the factor that significantly affects the linear ($p < 0.01$) and quadratic ($p < 0.01$) effects, along with the interactive effects ($p < 0.01$) of the SOR, as shown in Figure 1a. The response surface plot for the significant interactive effects also verified that the PDI decreased with increasing surfactant concentration and high HLB surfactant concentration, as shown in Figure 1b. Furthermore, significant interactive effects ($p < 0.05$) between the SOR and the PEG-40/PEG-60 hydrogenated castor oil ratio were also presented, along with significant interactive effects ($p < 0.05$) between the HLR and the PEG-40/PEG-60 hydrogenated castor oil ratio, as shown in Figure 1c.

The PDI, which represents the dispersion of the nanocarrier size distribution, is a highly significant physical characteristics to be considered when developing nanosystems, because the PDI attributes of the lipid-based particle can affect the characteristics, product efficacy, stability, and appearance of the formulation.

Table 4. Significance Probability of Regression Coefficients in the Final Model

type of effects	variables	droplet size (Y_1, nm)		PDI (Y_2)		entrapment efficiency (Y_3, %)	
		F-value	p-value	F-value	p-value	F-value	p-value
main effects	X_1	148.58	<0.0001	1.18	0.3030[a]	2982.05	<0.0001
	X_2	10.66	0.0085	18.25	0.0016	484.82	<0.0001
	X_3	3.75	0.0817[a]	0.6976	0.4231[a]	45.79	<0.0001
quadratic effects	X_1^2	25.22	0.0005	3.08	0.1099[a]	640.99	<0.0001
	X_2^2	6.62	0.0277	25.65	0.0005	50.78	<0.0001
	X_3^2	0.8976	0.3658[a]	0	0.9957[a]	0.7159	0.4173[a]
interaction effects	X_{12}	0.0292	0.8678[a]	21.23	0.0010	113.02	<0.0001
	X_{13}	0.0099	0.9228[a]	7.43	0.0214	0.0447	0.8369[a]
	X_{23}	0.0443	0.8375[a]	8.54	0.0152	0.027	0.8727[a]

[a]Indicates not significant at ($p > 0.05$).
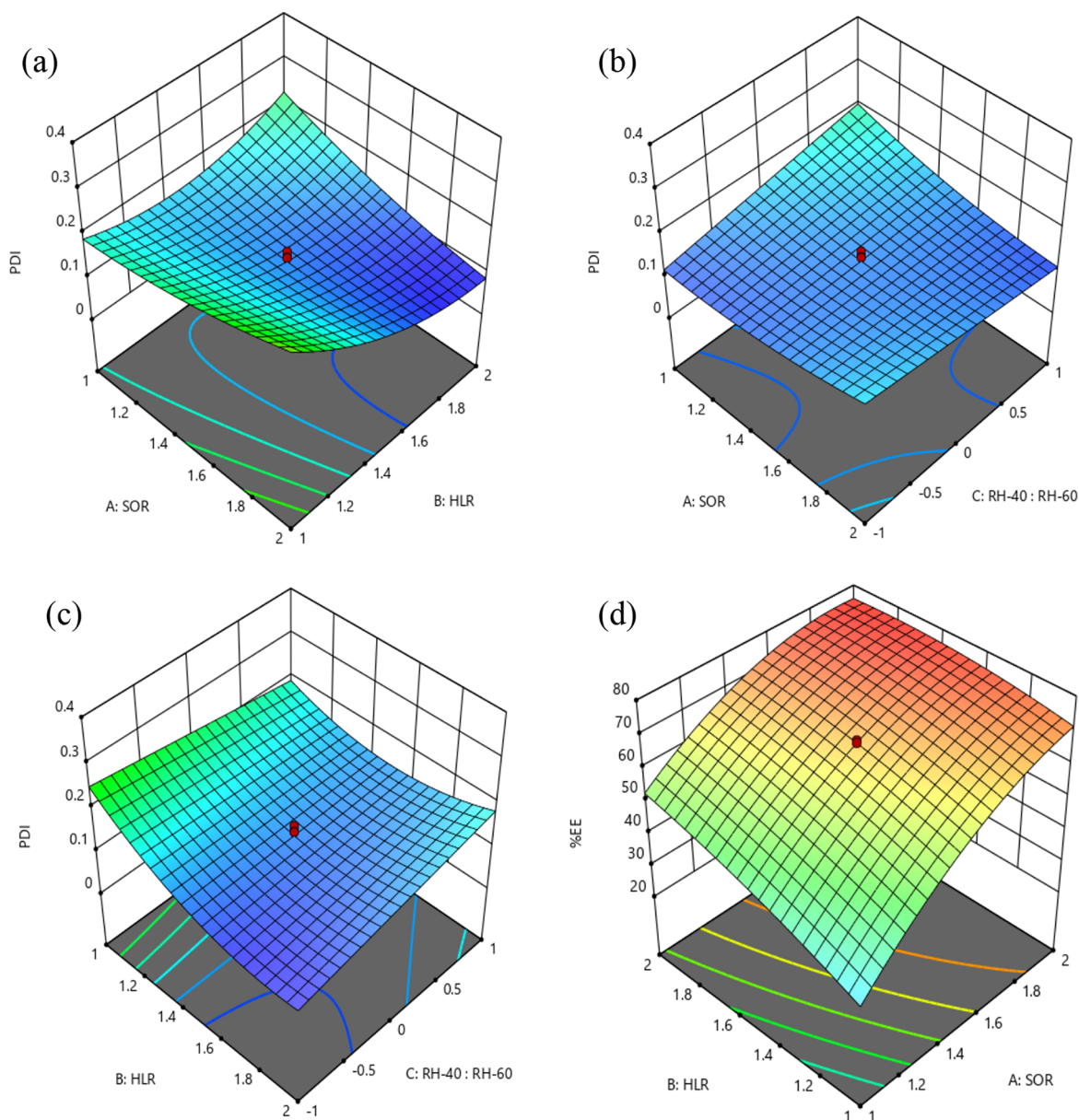
Figure 1. Response surface plots of the significant ($p < 0.05$) interaction effects on the studied variations; (a–c) PDI, (d) entrapment efficiency (%).

PDI values of 0.2 and lower are generally accepted in practice for nanoparticle materials.[15]

2.5.2.3. Entrapment Efficiency. The % EE of the TFE into the nanoemulsion in each run of experiments is presented in Table 5. The EE of the nanoemulsions was mostly affected by the SOR, which had a significant effect on the linear ($p <$ 0.0001), quadratic ($p <$ 0.0001), and interactive effects ($p <$ 0.0001), as shown in Table 4. Increasing the surfactant

Table 5. Different Responses of Optimization Experiments

run	droplet size (Y_1, nm) actual value	droplet size (Y_1, nm) predicted value	PDI (Y_2) actual value	PDI (Y_2) predicted value	entrapment efficiency (Y_3, %) actual value	entrapment efficiency (Y_3, %) predicted value
1	50.59	54.27	0.100	0.132	67.89	67.05
2	102.93	110.55	0.166	0.185	34.37	34.38
3	45.10	40.27	0.112	0.097	74.48	74.22
4	48.26	52.59	0.131	0.119	72.12	70.96
5	99.70	86.95	0.389	0.337	50.23	50.90
6	112.30	122.71	0.160	0.196	31.82	30.55
7	152.80	143.49	0.210	0.197	20.09	20.98
8	62.10	54.27	0.141	0.132	66.12	67.05
9	50.78	57.51	0.220	0.222	69.98	69.46
10	55.29	54.27	0.142	0.132	66.94	67.05
11	57.50	54.27	0.144	0.132	66.64	67.05
12	77.77	69.50	0.140	0.146	62.96	64.47
13	97.79	93.84	0.143	0.145	54.47	54.74
14	47.76	46.70	0.314	0.349	73.15	73.60
15	99.30	103.15	0.334	0.303	51.86	51.16
16	31.55	36.93	0.154	0.162	73.90	73.36
17	39.94	32.32	0.108	0.076	77.10	78.12
18	46.02	54.27	0.111	0.132	67.13	67.05
19	53.42	54.27	0.156	0.132	67.65	67.05
20	49.60	58.41	0.151	0.198	72.33	72.02

concentration resulted in an increased % EE, as shown in Figure 1d. Moreover, the HLR also contributed significantly to the linear ($p < 0.0001$) and quadratic ($p < 0.0001$) effects. The % EE increased as the high HLB surfactant concentration increased, as shown in Table 4. Another factor that significantly affected the EE was the linear ($p < 0.0001$) effect of the PEG-40/PEG-60 hydrogenated castor oil ratio. Increasing the concentration of PEG-40 hydrogenated castor oil in the formulation resulted in an increase in the % EE, as shown in Table 4. Polyethylene glycol (PEG) hydrogenated castor oil is a nonionic solubilizer and emulsifying agent obtained by reacting hydrogenated castor oil with ethylene oxide. It is the solubilizer normally selected to solubilize carrier oils, fragrance substances, and hydrophobic active ingredients.[16,17] The difference between PEG-40 and PEG-60 hydrogenated castor oil involves the average number of moles of ethylene oxide in the structure and the HLB value. PEG-40 hydrogenated castor oil contains 40 moles of ethylene oxide and has an HLB value between 14 and 16, while PEG-60 hydrogenated castor oil contains 60 moles of ethylene oxide and has an HLB value between 15 and 17.[16,17] Therefore, an increasing number of moles of ethylene oxide in the PEG hydrogenated castor oil structure, along with an increasing HLB value, could result in a decrease in the EE of the nanoemulsions.

2.5.3. Optimization of Responses for Formulation of TFE Nanoemulsions. The optimum TFE nanoemulsions (with a minimum droplet size, a PDI not higher than 0.2, and maximum EE) can be fabricated with a SOR of 2:1, indicating a surfactant concentration of 10.0% w/w, an HLR of 1.6:1, and a PEG-40/PEG-60 hydrogenated castor oil ratio of 2:1. Numerical optimization was conducted through Design-Expert software with a maximized desirability of 1. The predicted values for the droplet size, PDI, and % EE obtained from the numeric optimization are illustrated in Table 6.

The actual values derived from the experiment and the theoretical predicted values were statistically compared, as shown in Table 6. The percentage of prediction error was less

Table 6. Predicted and Actual Value of Responses at Optimized Conditions

response	predicted value	actual value	% prediction error
Y_1; droplet size (nm)	32.404	34.01	4.95
Y_2; PDI	0.153	0.150	2.00
Y_3; entrapment efficiency (%)	78.026	75.85	2.87

than 5% for all responses, indicating that the model was acceptable.

2.5.4. Morphology of TFE Nanoemulsions. In general, the droplet in the nanoemulsions had a spherical shape and consisted of a hydrophobic oil core surrounded by a thin interfacial layer consisting of a surfactant.[8] In this study, the morphology of the TFE nanoemulsions observed by transmission electron microscopy (TEM) also demonstrated a mostly spherical shape surrounded by the adsorbed surfactants, as shown in Figure 2.
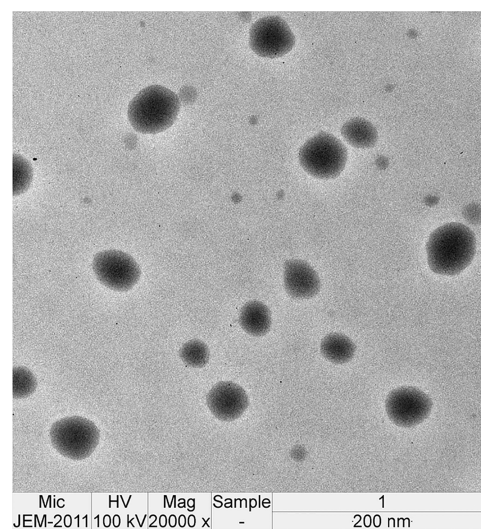
Figure 2. TEM of the TFE nanoemulsions.

3. CONCLUSIONS

Nanoemulsions containing TFE were successfully fabricated using the second degree polynomial model to optimize and explain the effects of independent variables, including the SOR, HLR, and PEG-40/PEG-60 hydrogenated castor oil ratio on the droplet size, PDI, and EE by a central composite design (CCD). TFE nanoemulsions with a minimum droplet size, a PDI not higher than 0.2, and maximum EE were obtained using numerical optimization. Numerical optimization was adopted to find the best formulating conditions, which were a SOR of 2:1, an HLR of 1.6:1, and a PEG-40/PEG-60 hydrogenated castor oil ratio of 2:1. Moreover, an in vitro study indicated that the TFE extracted by SFE possessed a potential scavenging activity against DPPH radicals and also had a great reducing power. Consequently, nanoemulsions containing TFE could be a valuable active substance for the further development of nutraceutical and cosmeceutical products.

4. MATERIALS AND METHODS

4.1. Chemical Materials. DPPH and TPTZ were purchased from Sigma-Aldrich Chemie GmbH (Schnelldorf, Germany).

FeSO$_4$•7H$_2$O and C$_2$H$_9$NaO$_5$ were purchased from Loba Chemie Pvt. Ltd. (Mumbai, India). Ethanol, FeCl$_3$·6H$_2$O, methanol, and hexane were purchased from Merck Ltd. (Darmstadt, Germany). Deionized water and sodium hydroxide were purchased from RCI Labscan Limited (Bangkok, Thailand). Polysorbate 80, PEG-40 hydrogenated castor oil, and PEG-60 hydrogenated castor oil were purchased from Chemecosmetics (Bangkok, Thailand).

4.2. Sample Preparation. Dried tea flowers were obtained from 101 Tea Co., Ltd., Mae Fa Luang District, Chiang Rai, Thailand, between September and October 2021. The dried tea flowers were ground using a grinder (Panasonic Co., Ltd., Osaka, Japan) to obtain a fine powder. The sample was kept in an air tight container.

4.3. Supercritical Fluid Extraction. The extraction of the tea flowers was carried out using SFE equipment (SFC-CO$_2$-4000 analytical system, JASCO Inc., Tokyo, Japan). For each experiment, 30 g of tea flower powder was placed in an SFE vessel. The flow rate of CO$_2$ and ethanol (a cosolvent) were both set to 1.0 mL/min, and the extraction was carried out using a pressure of 30 mPa. The extraction was performed in triplicate. The TFE was collected and stored in a container protected from light at 4 °C until required.[10,18,19]

4.4. Qualification of Polyphenolic Compounds.
4.4.1. TPC Determination. The TPC in the TFE was evaluated using the Folin–Ciocalteu reaction, which was slightly modified from the method of Myo et al.[20] and Theansungnoen et al.[21] In this study, gallic acid was used to prepare the standard curve. The absorbance was measured at 765 nm, and the TPC was expressed as mg GAE per gram of sample. All experiments were performed in triplicate.

4.4.2. TFC Determination. The TFC in the TFE was determined using a method slightly modified from the method of Myo et al.[20] and Theansungnoen et al.[21] Quercetin was used to prepare the standard curve. The absorbance was measured at 510 nm, and the TFC was expressed as mg QE per gram of sample. All experiments were performed in triplicate.

4.5. Determination of Bioactive Compounds.
4.5.1. UHPLC-ESI-QTOF-MS/MS Analysis. The TFE was analyzed using an UHPLC Agilent 1290 Infinity II System coupled to an Agilent 6545 LC-QTOF/MS. The separation was carried out using a Waters XBridge C18 (100 mm × 2.1 mm, 2.5 μm) column. The elution was achieved using a binary gradient system, with 0.1% formic acid in deionized water as eluent A and 0.1% formic acid in acetonitrile (ACN) as eluent B. The gradient steps were 5–17% B at 0–13 min, followed by 17–100% B at 13–20 min, 100% B at 20–25 min, and 100–5% B at 25–27 min, with a flow rate of 0.3 mL/min. Finally, a postrun was set to equilibrate the column for 6 min between analyses.

For the LC–MS system, a dual Agilent Jet System electrospray ionization (ESI) was used as an interface, with specific parameters including sheath gas temperature, 250 °C; sheath gas flow rate, 12 L/min; gas flow rate, 11 L/min; gas temperature, 300 °C; and nebulizer pressure, 45 psig. The LC–MS full-scan mode was operated using positive and negative ionizations. The scan range was 50–1050 m/z, and the scan rate was 1 spectra/s. Auto-MS^2 was managed using fixed collision energies of 10, 20, and 40 eV. The MS/MS scan range was set from 50 to 1100 m/z, with a scan rate of 3 spectra/s. The isolation width MS/MS was set at ±4 m/z. The reference solutions were incorporated to provide internal reference masses for mass correction in positive and negative modes of operation.[22,23]

4.5.2. UHPLC-ESI-QqQ-MS/MS Analysis. Bioactive compounds from the TFE were determined using a Shimadzu Nexera X2 UHPLC system (Kyoto, Japan) equipped with a CBM-20A controller, DGU-20A5R degasser, LC-30 AD binary gradient pumps, a SIL-30 AC autosampler, and a CTO-20 AC column oven. Each bioactive compound was analyzed using a C18 reversed-phase Avantor ACE Excel C18-PFP (100 mm × 2.1 mm, 1.7 μm) column. The injection volume was 1 μL. Elution was performed using a binary gradient system with eluent (A) 0.2% formic acid diluted in deionized water and eluent (B) ACN. The gradient steps were 10% B at 0–0.30 min, then 10–15% B at 0.30–2.40 min, 15–20% B at 2.40–3.25 min, 20% B at 3.25–3.60 min, 20–95% B at 3.60–6.20 min, 95% B at 6.20–7.00 min, 95–10% B at 7.00–7.50 min, and 10% B at 7.50–11.0 min, with a flow rate of 0.3 mL/min.

For MS detection, both positive and negative ionization modes were operated using a Shimadzu LCMS-8060 (Kyoto, Japan) equipped with an ESI source. A triple quadrupole system was used for detection, under multiple reaction monitoring (MRM) mode. Nitrogen was used as a drying and nebulizing gas, at a flow rate of 10.0 and 3.0 L/min, respectively. The heating gas flow rate was 10.0 L/min. The ESI temperature was set at 300 °C with the temperature of the DL and the heat block set at 250 and 400 °C, respectively. The bioactive compounds were characterized by comparing the precursor ions (m/z), product ions (m/z), and retention times (RT, min). LabSolutions software (Kyoto, Japan) was used to verify and process the bioactive compounds. The concentration of each compound was expressed as ppm compared to the standards.[20,24] The selected standard compounds are detailed in Table 7.

Table 7. List of Quantified Standard Compounds

compounds	[M − H] − (m/z)	product ion (m/z)	polarity
caffeine	195.00	138.15	positive
caffeic acid	178.80	135.20	negative
protocatechuic acid	153.25	109.05	negative
gallic acid	169.10	125.20	negative
p-coumaric acid	162.85	119.00	negative
ferulic acid	193.00	134.10	negative
catechin	289.25	245.20	negative
epicatechin (EC)	289.00	245.30	negative
gallocatechin (GC)	304.95	125.20	negative
epigallocatechin (EGC)	304.80	125.10	negative
catechin gallate (CG)	441.10	169.20	negative
gallocatechin gallate (GCG)	456.95	169.20	negative
epigallocatechin gallate (EGCG)	457.00	169.20	negative

4.6. Antioxidant Activity Assays. *4.6.1. DPPH Radical Scavenging Assay.* Diluted TFE concentrations were prepared in ethanol in order to determine the radical scavenging activity using the DPPH assay, which was slightly modified from Nantarat et al.[25] Gallic acid, ascorbic acid, and quercetin were used as the standards. Briefly, the TFE solution was incubated with 167 μM DPPH• in ethanol in the dark at room temperature for 30 min. The absorbance was measured at 517 nm using a spectrophotometer microplate reader (SPECTROstar Nano, Ortenberg, Germany). All experiments were performed in triplicate. The inhibiting effect of the TFE was calculated using the following equation:

$$\%\text{inhibition} = [(\text{Ac} - \text{As})/\text{Ac}] \times 100 \qquad (1)$$

where Ac is the absorbance of the blank and As is the absorbance of the test sample. The IC_{50} was then calculated using a calibration curve of the TFE by plotting the sample concentration and the % inhibition.

4.6.2. FRAP Assay. The FRAP values for the TFE were evaluated compared to standard ferrous sulfate solution, using a method that was slightly modified from Nantarat et al.[25] The TFE samples were prepared in ethanol and mixed with the FRAP reagent. The mixtures were then incubated for 5 min. The absorbance was measured at 593 nm. The FRAP values of each sample were calculated using the regression equation derived from the standard curve. The calibration curve was linear, with a regression coefficient (R^2) of 0.9999 (data not shown). All experiments were performed in triplicate.

4.7. Preparation of the TFE-Loaded Nanoemulsions. The TFE nanoemulsions were prepared using emulsion inversion point (EIP) methods. *Camellia sinensis* seed oil was selected as the oil phase, and propylene glycol dissolved in deionized water was selected as the continuous phase. In this study, PEG-40 hydrogenated castor oil, PEG-60 hydrogenated castor oil, and polysorbate 80 were selected as the surfactant system. Briefly, using a magnetic stirrer, the oil and surfactant were slowly mixed with an aqueous phase containing propylene glycol, Spectrastat BHL, and deionized water, at room temperature. Stirring was continued until the nanoemulsion was completely formed.[26]

4.8. Characterization of Nanoemulsions. *4.8.1. Droplet Size Analysis.* A zetasizer (Malvern Instruments Ltd., Malvern, UK) was used to analyze the nanoemulsion droplet size following a previous protocol.[26] Each formulation was diluted with water at a ratio of 1:100, at 25.0 ± 0.1 °C. All measurements were analyzed in triplicate. The size (nm) and size distribution (PDI) were reported.[26]

4.8.2. Entrapment Efficiency. The EE of each TFE nanoemulsion run was investigated using a centrifugal filtration device with a 100 kDa molecular weight cutoff filter (Microcon Millipore, Billerica, MA). Briefly, each formulation was added to the sample reservoir and then centrifuged at $1500 \times g$ at 4 °C for 30 min to separate the entrapped and untrapped components. The EE of the TFE nanoemulsion was evaluated using the Folin−Ciocalteu reaction to measure its TPC.[27] All experiments were analyzed in triplicate.

4.8.3. Morphology of Nanoemulsions by TEM. The morphology of the TFE nanoemulsions was investigated according to the method reported by Nantarat et al.[26] Each sample was prepared in a 300 mesh copper grid, and 2% phosphotungstic acid was used to adjust the contrast of the image. The derived sample was analyzed using a JEOL JEM-1200 EXII electron microscope (Japan) operated at 80 kV at 40,000× magnification.

4.9. Experimental Design. The effects of independent variables including X_1 (SOR), X_2 (HLR), and X_3 (the PEG-40/PEG-60 hydrogenated castor oil ratio) on Y_1 (droplet size), Y_2 (PDI), and Y_3 (EE) were studied using a response surface methodology (RSM) design. The coded independent variables are given in Table 8. CCD was applied along with the quadratic model.[28]

The second degree polynomial equation (as follows) was employed to express Y_1 (droplet size), Y_2 (PDI), and Y_3 (EE) as a function of the independent variables.

Table 8. Levels of Independent Variables

independent variables	coded level				
	axial $(-\alpha)$	low	center	high	axial $(+\alpha)$
surfactant-to-oil ratio (SOR) (X_1)	0.6591	1	1.5	2	2.3409
the ratio of high HLB surfactant to low HLB surfactant; HLR (X_2)	0.6591	1	1.5	2	2.3409
the effect of PEG-40 and PEG-60 hydrogenated castor oil; RH-40:RH-60 (X_3)	−1.68	−1	0	1	1.68

$$Y_i = \beta_0 + \beta_1 X_1 + \beta_2 X_2 + \beta_3 X_3 + \beta_{11} X_1^2 + \beta_{22} X_2^2 + \beta_{33} X_3^2$$
$$+ \beta_{12} X_1 X_2 + \beta_{13} X_1 X_3 + \beta_{23} X_2 X_3$$

where Y_i represents the responses, β_0 indicates a constant, and β_i, β_{ii}, and β_{ij} are linear, quadratic, and interactive coefficients, respectively. The coefficients were provided using Design-Expert software (version 7.1; Stat-Ease Inc., Minneapolis, MN, USA).

4.10. Statistical Analysis. The experimental procedure and analysis were carried out in triplicate. The results were analyzed using one-way ANOVA with 95% confidence level ($p < 0.05$). The data are shown as the mean $\pm$ standard deviation.

■ AUTHOR INFORMATION

Corresponding Author

  Nara Yaowiwat − *School of Cosmetic Science and Green Cosmetic Technology Research Group, School of Cosmetic Science, Mae Fah Luang University, Chiang Rai 57100, Thailand;* ⦿ orcid.org/0000-0002-7272-6973; Email: nara.nan@mfu.ac.th

Authors

  Worrapan Poomanee − *Department of Pharmaceutical Sciences, Faculty of Pharmacy, Chiang Mai University, Chiang Mai 50200, Thailand*

  Pimporn Leelapornpisid − *Department of Pharmaceutical Sciences, Faculty of Pharmacy, Chiang Mai University, Chiang Mai 50200, Thailand;* ⦿ orcid.org/0000-0003-1273-7336

  Phanuphong Chaiwut − *School of Cosmetic Science and Green Cosmetic Technology Research Group, School of Cosmetic Science, Mae Fah Luang University, Chiang Rai 57100, Thailand*

Complete contact information is available at:
https://pubs.acs.org/10.1021/acsomega.3c00602

Notes

The authors declare no competing financial interest.

■ REFERENCES

(1) Chen, D.; Chen, G.; Sun, Y.; Zeng, X.; et al. Physiological genetics, chemical composition, health benefits and toxicology of tea (*Camellia sinensis* L.) flower: A review. *Food Res. Int.* **2020a**, *137*, No. 109584.

(2) Chen, D.; Ding, Y.; Chen, G.; Sun, Y.; et al. Components identification and nutritional value exploration of tea (*Camellia sinensis* L.) flower extract: Evidence for functional food. *Food Res. Int.* **2020b**, *132*, No. 109100.

(3) Zhao, B. Antioxidant effects of green tea polyphenols. *Chin. Sci. Bull.* **2003**, *48*, 315−319.

(4) Grzesik, M.; Naparło, K.; Bartosz, G.; Sadowska-Bartosz, I. Antioxidant properties of catechins: Comparison with other antioxidants. *Food Chem.* **2018**, *241*, 480−492.

(5) Bratovcic, A.; Suljagic, J. Micro-and nano-encapsulation in food industry. *Croat. J. Food Sci.* **2019**, *11*, 113−121.

(6) Cerda-Opazo, P.; Gotteland, M.; Oyarzun-Ampuero, F. A.; Garcia, L. Design, development and evaluation of nanoemulsion containing avocado peel extract with anticancer potential: A novel biological active ingredient to enrich food. *Food Hydrocolloids* **2021**, *111*, No. 106370.

(7) Ezhilarasi, P. N.; Karthik, P.; Chhanwal, N.; Anandharamakrishnan, C. Nanoencapsulation techniques for food bioactive components: a review. *Food Bioprocess. Technol.* **2013**, *6*, 628−647.

(8) McClements, D. J. *Nanoparticle-and microparticle-based delivery systems: Encapsulation, protection and release of active compounds*; CRC press, 2014.

(9) Livney, Y. D. Nanoencapsulation technologies. In *Engineering foods for bioactives stability and delivery*; Springer: New York, NY, 2017; pp 143−169.

(10) Chen, Z.; Mei, X.; Jin, Y.; Kim, E. H.; et al. Optimisation of supercritical carbon dioxide extraction of essential oil of flowers of tea (*Camellia sinensis* L.) plants and its antioxidative activity. *J. Sci. Food Agric.* **2014**, *94*, 316−321.

(11) Legeay, S.; Rodier, M.; Fillon, L.; Faure, S.; et al. Epigallocatechin gallate: a review of its beneficial properties to prevent metabolic syndrome. *Nutrients* **2015**, *7*, 5443−5468.

(12) Girsang, E.; Lister, I. N. E.; Ginting, C. N.; Sholihah, I. A.; et al. Antioxidant and antiaging activity of rutin and caffeic acid. *Pharmaciana* **2020**, *10*, 147.

(13) Luiz, M. T.; Viegas, J. S. R.; Abriata, J. P.; Viegas, F.; et al. Design of experiments (DoE) to develop and to optimize nanoparticles as drug delivery systems. *Eur. J. Pharm. Biopharm.* **2021**, *165*, 127−148.

(14) Mehmood, T.; Ahmad, A.; Ahmed, A.; Ahmed, Z. Optimization of olive oil-based O/W nanoemulsions prepared through ultrasonic homogenization: A response surface methodology approach. *Food Chem.* **2017**, *229*, 790−796.

(15) Danaei, M.; Dehghankhold, M.; Ataei, S.; Hasanzadeh Davarani, F.; et al. Impact of particle size and polydispersity index on the clinical applications of lipidic nanocarrier systems. *Pharmaceutics* **2018**, *10*, 57.

(16) Burnett, C. L.; Heldreth, B.; Bergfeld, W. F.; Belsito, D. V.; et al. Safety Assessment of PEGylated oils as used in cosmetics. *Int. J. Toxicol.* **2014**, *33*, 13S−39S.

(17) Jang, H. J.; Shin, C. Y.; Kim, K. B. Safety evaluation of polyethylene glycol (PEG) compounds for cosmetic use. *Toxicology* **2015**, *31*, 105−136.

(18) Ameer, K.; Chun, B. S.; Kwon, J. H. Optimization of supercritical fluid extraction of steviol glycosides and total phenolic content from *Stevia rebaudiana* (Bertoni) leaves using response surface methodology and artificial neural network modeling. *Ind. Crops Prod.* **2017**, *109*, 672−685.

(19) Dhakane-Lad, J.; Kar, A. Supercritical CO_2 extraction of lycopene from pink grapefruit (*Citrus paradise* Macfad) and its degradation studies during storage. *Food Chem.* **2021**, *361*, No. 130113.

(20) Myo, H.; Nantarat, N.; Khat-Udomkiri, N. Changes in bioactive compounds of coffee pulp through fermentation-based biotransformation using Lactobacillus plantarum TISTR 543 and its antioxidant activities. *Fermentation* **2021**, *7*, 292.

(21) Theansungnoen, T.; Nitthikan, N.; Wilai, M.; Chaiwut, P.; et al. Phytochemical Analysis and Antioxidant, Antimicrobial, and Antiaging Activities of Ethanolic Seed Extracts of Four Mucuna Species. *Cosmetics* **2022**, *9*, 14.

(22) Astiti, M. A.; Jittmittraphap, A.; Leaungwutiwong, P.; Chutiwitoonchai, N.; et al. LC-QTOF-MS/MS based molecular networking approach for the isolation of α-glucosidase inhibitors and virucidal agents from *Coccinia grandis* (L.) Voigt. *Foods* **2021**, *10*, 3041.

(23) Mocan, A.; Moldovan, C.; Zengin, G.; Bender, O.; et al. UHPLC-QTOF-MS analysis of bioactive constituents from two Romanian Goji (*Lycium barbarum* L.) berries cultivars and their antioxidant, enzyme inhibitory, and real-time cytotoxicological evaluation. *Food Chem. Toxicol.* **2018**, *115*, 414−424.

(24) Cheng, H.; Wu, W.; Chen, J.; Pan, H.; et al. Establishment of anthocyanin fingerprint in black wolfberry fruit for quality and geographical origin identification. *LWT* **2022**, *157*, No. 113080.

(25) Nantarat, N.; Mueller, M.; Lin, W. C.; Lue, S. C.; et al. Sesaminol diglucoside isolated from black sesame seed cake and its antioxidant, anti-collagenase and anti-hyaluronidase activities. *Food Biosci.* **2020**, *36*, No. 100628.

(26) Nantarat, T.; Chansakaow, S.; Leelapornpisid, P. Optimization, characterization and stability of essential oils blend loaded nano-emulsions by PIC technique for anti-tyrosinase activity. *Int. J. Pharm. Pharm.* **2015**, *7*, 308−312.

(27) Sari, T. P.; Mann, B.; Kumar, R.; Singh, R. R. B.; et al. Preparation and characterization of nanoemulsion encapsulating curcumin. *Food Hydrocolloids* **2015**, *43*, 540−546.

(28) Poomanee, W.; Khunkitti, W.; Chaiyana, W.; Leelapornpisid, P. Optimization of *Mangifera indica* L. kernel extract-loaded nano-emulsions via response surface methodology, characterization, stability, and skin permeation for anti-acne cosmeceutical application. *Pharmaceutics* **2020**, *12*, 454.